

GC-MS metabolite and transcriptome analyses reveal the differences of volatile synthesis and gene expression profiling between two Chinese rose cultivars

Kaiqing Luo^{1#}, Chao Song^{1,2#}, Tingting Bao¹, Rui Huang^{1,3}, Shengnan Lin^{1,2}, Yingxue Yang^{1,2}, Luhong Leng¹, Xuezhu Liao¹, Cuihua Gu^{4*}, Zhiqiang Wu^{1,2*} and Xiaoni Zhang^{1,2*}

¹ Shenzhen Branch, Guangdong Laboratory of Lingnan Modern Agriculture, Key Laboratory of Synthetic Biology, Ministry of Agriculture and Rural Affairs, Agricultural Genomics Institute at Shenzhen, Chinese Academy of Agricultural Sciences, Shenzhen 518120, China

² Kunpeng Institute of Modern Agriculture at Foshan, Foshan 528000, China

³ College of Horticulture, Shanxi Agricultural University, Jinzhong 030031, China

⁴ College of Landscape and Architecture, Zhejiang Agriculture and Forestry University, Hangzhou 311300, China

Authors contributed equally: Kaiqing Luo, Chao Song

* Corresponding authors, E-mail: gucuihua@zafu.edu.cn; wuzhiqiang@caas.cn; zhangxiaoni@caas.cn

Abstract

Floral fragrance is an important ornamental trait of horticultural crops. However, research on the physiological and molecular biology of the floral volatile compounds in Chinese rose is limited. This study conducted metabolomic and transcriptomic analyses on the floral volatile compounds of *Rosa chinensis* (*R. chinensis*) 'Old Blush' ('OB') and *R. chinensis* 'Chilong Hanzhu' ('CH'). A total of 22 major volatile organic compounds (VOCs) were detected in the blooming flowers of 'OB' and 'CH'. The main VOCs emitted from 'OB' petals was 1,3,5-trimethoxybenzene (TMB), while that from 'CH' petals was 2-phenylethanol (2-PE). The GO and KEGG enrichment on differentially expressed genes (DEGs) revealed the essential role of phenylpropanoid pathway in the difference of floral fragrance between two cultivars, and a total of 15 key genes involved in the biosynthesis of phenylpropanoid were identified in *R. chinensis* flowers. The overexpression of *RcCH_AADC-1* in transgenic tobacco plants led to the accumulation of 2-PE. In contrast, no significant change in the level of 2-PE was observed after the transient transformation of *RcCH_PAR1* or *RcCH_PAR1_Like* into tobacco plants. These findings provide valuable insight for enhancing the accumulation of 2-PE in *R. chinensis*.

Citation: Luo K, Song C, Bao T, Huang R, Lin S, et al. 2025. GC-MS metabolite and transcriptome analyses reveal the differences of volatile synthesis and gene expression profiling between two Chinese rose cultivars. *Ornamental Plant Research* 5: e009 <https://doi.org/10.48130/opr-0025-0003>

Introduction

Roses are one of the most popular cut flowers and have been cultivated all over the world for more than 2,000 years, containing 200 species and 35,000 cultivars^[1], being both an important ornamental plant and a crucial oil crop. For centuries, roses have been used as a raw material for natural fragrances and oil^[2], also known as 'liquid gold'. In addition, roses have other economic benefits for humans, such as being used as food, pies, tea, medicine, creams, and crafts^[3]. *Rosa gigantea*, *R. chinensis* 'Hume's Blush Tea-scented China', 'Parks' Yellow Tea scented China', 'Old Blush', and 'Chilong Hanzhu' are among the most important progenitors in the cultivation of modern roses^[4,5]. Previous studies have found that the Chinese rose is rich in distinctive fragrance, while various modern roses lack fragrance diversity due to breeders' emphasis on the appearance of roses rather than fragrance during the long history of traditional cross-breeding^[1,6]. Hence, increasing the fragrance diversity in roses can not only improve their performance as an ornamental flower but also promote their economic benefits.

Plants emit a variety of volatile organic compounds (VOCs) from different tissues (such as roots, leaves, and fruits), and flowers were found to be an important apparatus that releases the highest amounts and diversity of VOCs^[7–9]. Based on their biosynthetic origin, floral VOCs can be divided into three major classes, terpenoids, phenylpropanoids/benzenoids, and fatty acid derivatives^[8,10]. Recently, there has been a growing emphasis on the study of genes related to the VOCs' biosynthesis in *Clarkia breweri* (*C. breweri*),

Antirrhinum majus (*A. majus*), *Arabidopsis thaliana* (*A. thaliana*), *Petunia hybrida* (*P. hybrida*), and *Rosa*. For example, terpene synthases (TPSs) have been confirmed to participate in the formation of monoterpenes such as linalool, (*E*)- β -ocimene, germacrene D, and other terpenoids in *C. breweri*, *A. majus*, *A. thaliana*, and *R. hybrida*^[11–15]. In petunia, phenylacetaldehyde synthase (PAAS), as a member of the aromatic amino acid decarboxylase (AADC) family^[16–18], catalyzes the formation of phenylacetaldehyde (PALd), which is a precursor for the synthesis of 2-phenylethanol (2-PE)^[16]. In the biosynthesis of phenylpropanoid compounds, O-methyltransferases play an essential role in important phenylpropanoid VOCs, such as 3,5-dimethoxytoluene (DMT) and 1,3,5-trimethoxybenzene (TMB) in rose^[19,20], and methyleugenol and isomethyleugenol in *C. breweri*^[21].

The fragrance of rose is primarily composed of monoterpene alcohols, including 2-PE, citronellol, geraniol, nerol, and acetate derivatives^[22]. The 2-PE, a significant floral compound in roses, plays a crucial role in the production of perfumery and essential oils^[20]. The concentration of 2-PE showed significant variability among different rose species. *R. multiflora* and *R. damascena* were demonstrated with elevated levels of 2-PE, whereas cultivars in *R. chinensis* ('Hermosa', 'Miss Lowe', and 'Semperflorens') and modern rose ('Papa Meiland') were observed with trace amounts of 2-PE emitted from petals^[23]. In the biosynthesis of 2-PE, two key enzymes, aromatic amino acid aminotransferase (AAAT) and phenylpyruvate decarboxylase (PPDC), are shown to be responsible for 2-PE production based on L-Phe via phenylpyruvic acid (PPA)^[24,25]. In

rose, the key enzymes involved in the biosynthesis of 2-PE were identified, including the enzymatic actions of AADC and phenylacetaldehyde reductase (PAR)^[17,26]. The overexpression of AADC, AAAT, and PAR genes resulted in an elevation of 2-PE content in *Solanum lycopersicum* (*S. lycopersicum*)^[27,28], and AADC, AAAT in *R. rugosa* 'Tanghong'^[29]. Hence, investigating the control of 2-PE biosynthesis and release in rose is crucial for understanding this process.

In this study, we selected *R. chinensis* 'Old blush' ('OB') which has a light fragrance and pink petals, and *R. chinensis* 'Chilong Hanzhu' ('CH') which has intensely fragrant and red petals as materials. We identified differentially abundant volatiles in the petals of 'OB' and 'CH' by gas chromatography-mass spectrometry (GC-MS). Combining transcriptomics analysis, we identified key genes involved in the floral fragrance biosynthesis pathway of *R. chinensis*. Further confirmation by performing transient transformation of key genes in tobacco leaves uncovered their contribution to the accumulation of 2-PE. These new findings provide a theoretical basis for molecular breeding of Chinese rose fragrance.

Materials and methods

Plant materials

Two rose germplasm resources, *R. chinensis* 'OB' and *R. chinensis* 'CH', were cultivated in the same greenhouse under natural conditions in Shenzhen Comprehensive Experimental Base, Chinese Academy of Agricultural Sciences, Guangdong Province, China (22.60° N, 114.51° E). The flowers were divided into three developmental stages: green flower buds (S1), flower buds with petals beginning to change color (S2), and full blooming flowers (S3), according to previous research^[30,31]. For *in vivo* bioassay of RcCH_AADC1, RcCH_PAR1, and RcCH_PAR1_Like recombinant proteins, *Nicotiana benthamiana* (*N. benthamiana*) plants were grown in a greenhouse at 22 °C under a light/dark period of 16 h/8 h, light intensity of 200 $\mu\text{mol}\cdot\text{m}^{-2}\cdot\text{s}^{-1}$ and relative humidity of 60%. The young leaves of 4-week-old *N. benthamiana* were used for *Agrobacterium tumefaciens* (*A. tumefaciens*) infiltration experiments.

The GC-MS based profiling of VOCs in *R. chinensis*

The collection of floral scent was performed according to a previous study^[32]. Briefly, the fresh rose flowers were excised from plants, and approximately 0.7 g of flower samples were transformed into a collection bottle. Four independent replicates were performed at the S3 stage of *R. chinensis* 'OB' and 'CH' petals. The solid-phase microextraction was conducted to collect floral metabolites and the extracts were injected into GC-MS (QP-2010, Shimadzu, Japan) for identifying VOCs with a setup as described previously^[31]. After obtaining the chromatograms and mass spectrograms of floral compounds, their qualitative analysis was performed by searching the mass spectral and retention index (RI) against the National Institute of Standards and Technology (NIST, USA). The final relative contents of detected metabolites were based on the percentage of the peak area of selected mass to the total peak area of detected metabolites. The VOCs with an area of > 1% in 'OB' and 'CH' were considered to be the predominant VOCs of that sample. The odor of detected floral compounds were annotated according to the description from public website Flavornet (www.flavornet.org).

Transcriptome analysis

The raw RNA sequencing data of different flower stages of 'CH' and 'OB' were obtained from a previous study^[31] and public database NCBI (PRJNA351281 and PRJNA546486), respectively. Those datasets include nine (three biological replications for each stage) and six samples (two biological replications for each stage) for 'CH'

and 'OB', respectively. Quality control was performed using Fastqc v0.11.9, adapter and low-quality reads (Q < 20) were removed using Trimmomatic^[33]. The clean reads were mapped to the *R. chinensis* 'CH' reference genome using HISAT2 v2.2.1^[34], and the mapped reads were assembled using StringTie v2.1.6^[35] and expression levels were predicted. The read counts of these samples were calculated using HTSeq^[36] and used for differential gene expression analysis.

The gene expression level was evaluated by fragments per kilobase of transcript per million mapped fragments (FPKM). Transcripts with FPKM values of > 1 in at least one sample were defined as the threshold expression of that gene. Differential expression genes (DEGs) between two cultivars at different developmental stages (OB-S1 vs CH-S1, OB-S2 vs CH-S2, and OB-S3 vs CH-S3) was obtained using DESeq2 of TBtools-II v2.086^[37]. The $|\log_2(\text{Fold Change})| \geq 1$ and adjusted *p*-value < 0.05 were set as the criteria for screening DEGs. Principal component analysis (PCA) and correlation analysis matrix were conducted using online tools of Metware Cloud (<https://cloud.metware.cn>, accessed on 1 January 2024). Identification of DEGs, gene ontology (GO) analysis, and Kyoto Encyclopedia of Genes and Genomes (KEGG) pathway enrichment analysis were performed (*p* value < 0.05). Combined analyses of DEG functions and expression levels were conducted with MapMan 3.6.0RC1, which is a user-driven tool that visualizes large datasets as diagrams of metabolic pathways or other processes. The function annotations of DEGs derived from MapMan were visualized as a network using Cytoscape 3.10.1.

Gene cloning and sequence analysis

Total RNA was extracted from 'CH' flowers using a FastPure® Universal Plant Total RNA Isolation Kit (Vazyme, Nanjing, China) according to the manufacturer's instructions. First-strand cDNA was then synthesized using a HiScript® III 1st Strand cDNA Synthesis Kit (+gDNA wiper) (Vazyme, Nanjing, China) according to the manufacturer's instructions.

The motif identification of amino acid sequences for RcCH_AADC1, RcCH_PAR1, and RcCH_PAR1_Like was conducted using MEME (<https://meme-suite.org/meme/index.html>). The NCBI Conserved Domain Database (www.ncbi.nlm.nih.gov/cdd) was used to identify domains from the amino acid sequences of RcOB_OOMT1, RcOB_OOMT2, RcCH_OOMT1 and RcCH_OOMT2. The amino acid sequences of above-mentioned candidate genes from *R. chinensis*, *R. wichuraiana* Basye's Thornless, *R. rugosa*, *R. damascene*, *R. hybrida*, *Fragaria vesca* (*F. vesca*), *P. hybrida*, *S. lycopersicum*, and *Eucalyptus gunnii* were aligned using ClustalW and the neighbor-joining (NJ) trees were generated using Molecular Evolutionary Genetics Analysis, version 7 (MEGA, version 7). The bootstrap values were obtained with 1,000 replications. The motifs and trees were drawn with Chiplot^[38].

Transient transformation in tobacco leaves

The full-length CDS of RcCH_AADC1, RcCH_PAR1, and RcCH_PAR1_Like were amplified from the cDNA of *R. chinensis* 'CH' using designed primers (Supplementary Table S1). The candidate genes were inserted into vector pEAQ-HT. The pEAQ-HT vector with the target gene was introduced into *A. tumefaciens* strain GV3101^[39]. The positive colonies were collected and re-dissolved in the buffer containing 10 mM 2-(*N*-morpholino) ethanesulfonic acid (MES), 10 mM MgCl₂, and 200 μM acetosyringone (AS) and adjusted to OD600 of 0.8. After 2 h of incubation, the suspensions were pressure infiltrated into 4-week-old *N. benthamiana* leaves. After infiltration for 4 d, 1 g infected leaves were collected and placed in enclosed bottles for volatile compound analysis. The pEAQ-HT with empty vector was used as a negative control. The compound of 2-PE served as positive control.

Results

GC-MS-based VOCs profile of 'OB' and 'CH'

The two rose cultivars used in this study showed similar phenotype of double-petal flowers, and both cultivars bloom in all seasons (Supplementary Table S2). Some differences were observed in the flower color and size that 'OB' displays larger flowers than 'CH' (Fig. 1a & b; Supplementary Table S2).

To clarify the floral characteristics of 'OB' and 'CH', we performed GC-MS-based VOC profiling on the flower at the S3 stage of 'OB' and 'CH' (Fig. 1c, d). A total of 22 primary floral components (area > 1%) were identified either in 'OB' or 'CH', including 14 terpenoids, five fatty acid derivatives, three phenylpropanoids and their derivatives. The primary floral components of 'OB' and 'CH' accounted for 74.90% and 88.52% of total VOCs, respectively (Supplementary Table S3). Considering 22 primary floral components, terpenoids were found to be the most abundant VOC group (57%) emitted from the 'OB' flower, whereas in 'CH' flower the phenylpropanoids were the major VOC group (60%) compared with other VOC groups (Fig. 2a). Among the primary VOCs, 12 VOCs showed significant ($p < 0.05$) differences in their contents between two cultivars (Fig. 2b). Specifically, 2-PE and TMB were observed with the greatest variations between 'OB' and 'CH' (Fig. 2c). The content of 2-PE in 'CH' was accumulated significantly higher ($p < 0.05$) than in 'OB', while the trend in the content of TMB was reversed between the two cultivars (Fig. 2b).

With respect to the aroma odor, the two cultivars also exhibited a diversity of aroma types. Twenty two major VOCs have been classified into eight groups based on their fragrance descriptions following a previous report^[40]. These groups consist of herbal green, fresh green, damask sweet, fruity floral, tea fenolic, tea violet, woody honey, and others (Fig. 2d). The dominant flavor profile of 'OB' flowers was woody honey, characterized by a high presence of

terpenes and dihydro- β -ionol. The 'OB' flower contained another type of aroma, a tea scent, associated with TMB. In contrast, 'CH' flowers emitted a pronounced damask sweet scent predominantly composed of 2-PE, accounting for approximately 51.03% of total VOCs.

Analysis of the DEGs in *R. chinensis* flowers at different stages

To investigate the molecular basis for the metabolic differences between 'OB' and 'CH', we conducted a transcriptomic analysis of both cultivars at different developmental stages of flowers (S1–S3). PCA score plot based on gene expressions revealed a great variation between cultivars as two cultivars widely separated from each other. In addition, a notable separation was observed between S3 and the other two stages (S1–S2) in both 'OB' and 'CH' (Fig. 3a). Both PCA and correlation analysis demonstrated excellent repeatability among biological replicates (Fig. 3a, b). By comparing the gene expression profiles between two cultivars at different stages, a total of 1,899 (879 up-regulated and 1,020 down-regulated), 1,535 (702 up-regulated and 833 down-regulated), and 3,663 DEGs (1,767 up-regulated and 1,896 down-regulated) were identified in the comparisons of OB-S1 vs CH-S1, OB-S2 vs CH-S2, and OB-S3 vs CH-S3, respectively (Fig. 3c). The results of GO and KEGG enrichment analyses based on DEGs revealed the gene functions primarily in metabolism, chaperones, and folding catalysts, signal transduction, and biosynthesis of other secondary metabolites (Supplementary Fig. S1). As the flower at the S3 stage displayed the greatest variation in gene expression and VOC contents, we used MapMan to cluster the genes involved in the same metabolism using the DEGs that were associated with secondary metabolism at the S3 stage. A total of 155 genes were obtained and fed into MapMan for further analysis. Those DEGs were clustered into 18 different metabolism pathways, and they were mainly associated with flavonoids, isoprenoids, and phenylpropanoids biosynthesis, linking 52, 32, and 25 DEGs (Fig. 3d).

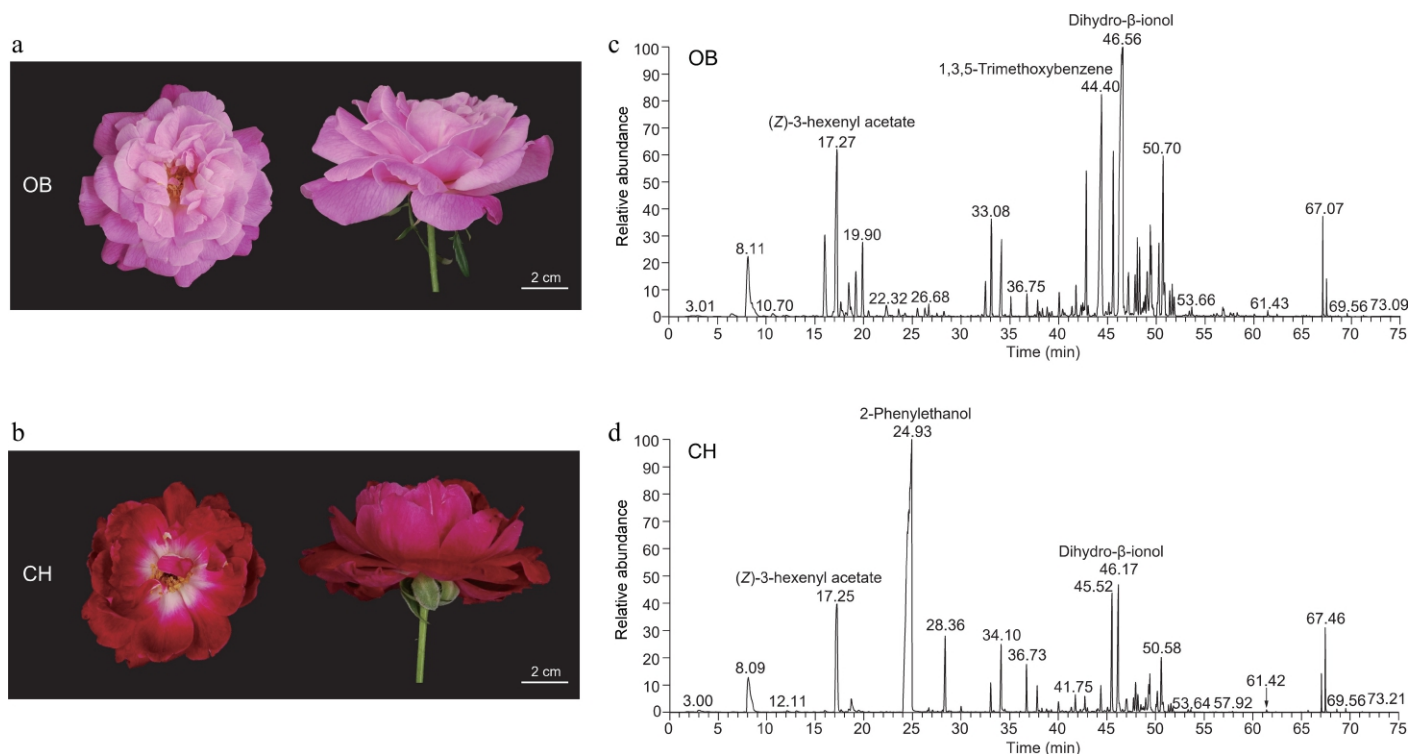


Fig. 1 Flower phenotypes and volatile compounds of 'OB' and 'CH'. (a), (b) Floral phenotypes of (a) 'OB', and (b) 'CH' at S3 (full opening stage). (c), (d) Chromatograms for the S3 petals of (c) 'OB', and (d) 'CH'. The three highest peaks were labeled with annotations in chromatograms of two cultivars.

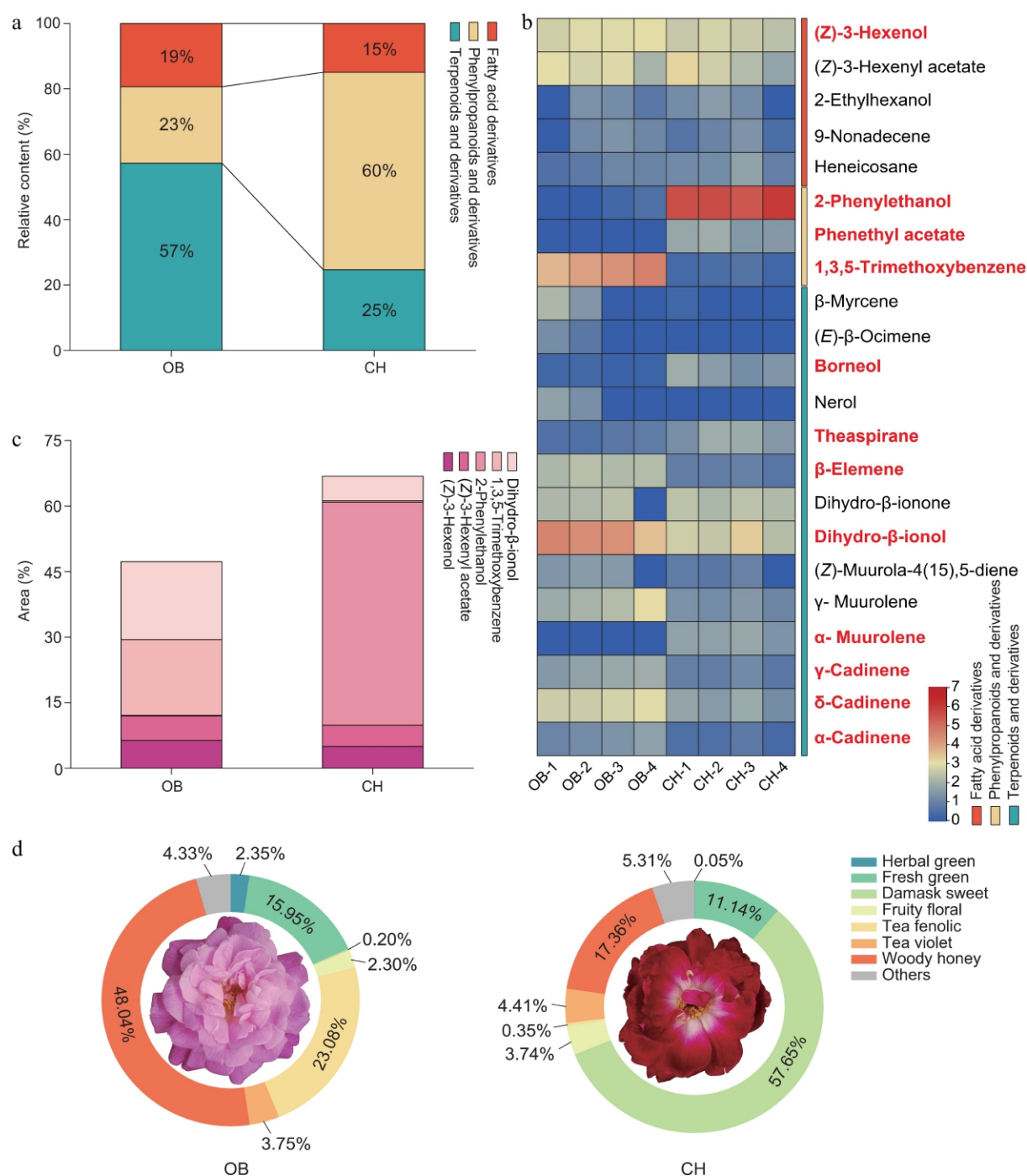


Fig. 2 The main VOCs of 'OB' and 'CH'. (a) Relative content of VOCs in different scent components of two cultivars. (b) Heatmap showed the relative content (log2-transformed peak area) of 22 major floral fragrance components. The text in bold and red indicates the significantly changed VOCs. (c) Area of the top five VOCs. (d) Classification of the aroma types of 'OB' and 'CH'.

Pathways analysis for floral fragrance between 'OB' and 'CH'

The blooming flowers (S3) of 'OB' and 'CH' were characterized by some typical floral VOCs, with TMB identified as the predominant aroma compound in 'OB' flowers and 2-PE as the key VOC in 'CH' flowers. The MapMan results indicate that the DEGs associated with phenylpropanoid pathway significantly contribute to the floral fragrance of the two cultivars (Fig. 3d). Based on these results and previous research, we identified 15 key structural genes related to phenylpropanoids biosynthesis in rose (Supplementary Table S4 & Fig. 4). There were two *phloroglucinol O-methyltransferase* (POMT) and

four *orcinol O-methyltransferases* (OOMT) genes within the biosynthetic pathway of TMB, and one *AAAT*, four *AADC*, five *PPDC*, and two *PAR* genes related to the biosynthesis of 2-PE. Among them, the *RcPOMT* gene was highly expressed at the S1 and S2 stages, followed by a decrease at the S3 stage of two cultivars. In contrast to *POMTs*, the *OOMTs* genes showed variations in expression patterns. The *OOMTs* of 'OB', *RcOB_OOMT1* (*RcCH_v1.0_chr2.3178*), and *RcOB_OOMT2* (*RcCH_v1.0_chr2.2828*), exhibited their highest expression levels exclusively at the S3 stage, whereas the *RcCH_OOMTs* genes of 'CH' remained unexpressed in flowers across all three stages. The expression of *RcCH_OOMT1* was observed primarily in the root and

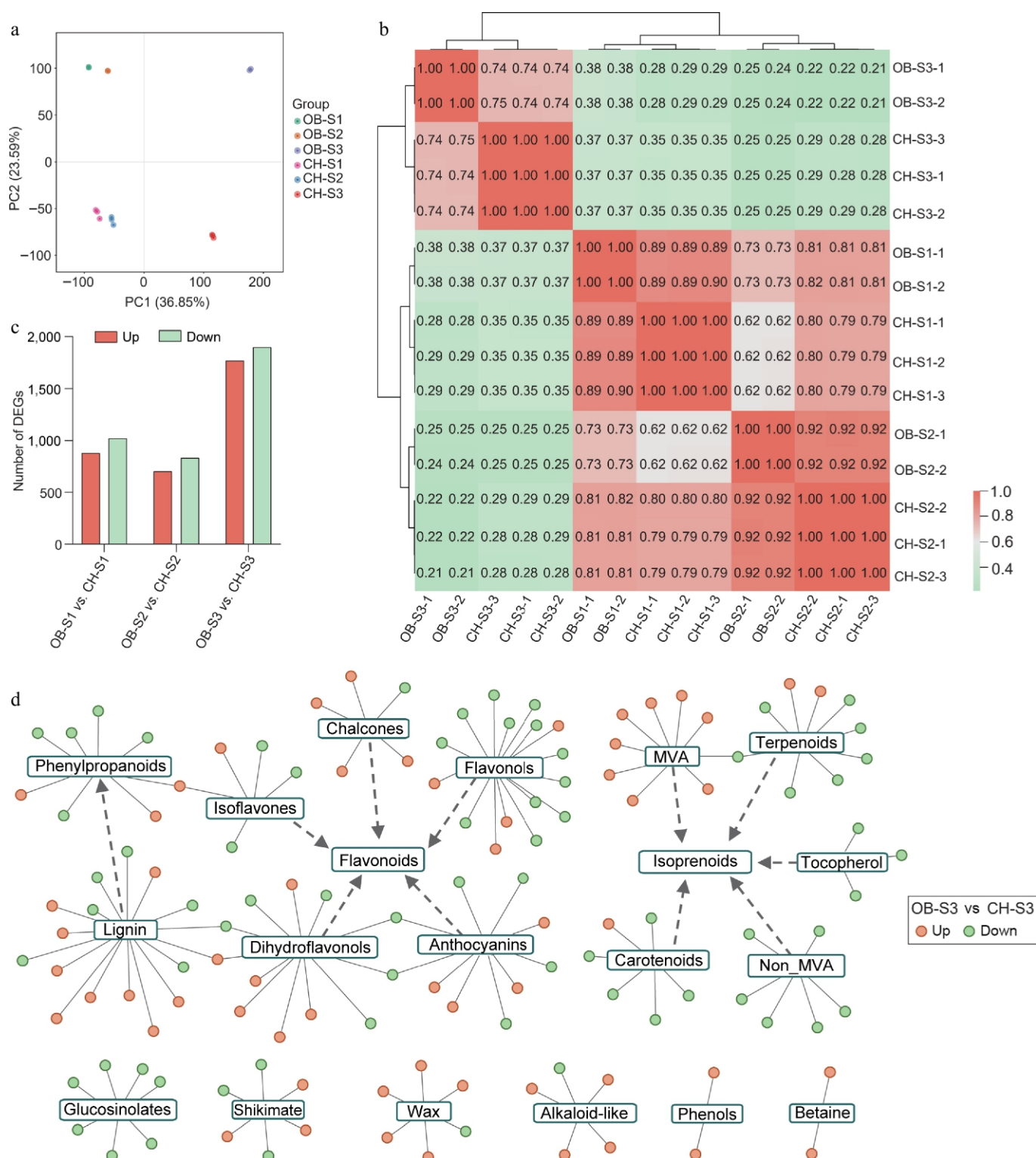


Fig. 3 Analysis of transcriptomes of 'OB' and 'CH' at S1–S3. (a) PCA showing the clustering of transcriptome of floral development stages (S1–S3) in *R. chinensis* petals. (b) Correlation analysis matrix among 'OB' and 'CH' at different development stages based on transcriptomes. (c) Statistics of DEGs in the comparisons of 'OB' and 'CH'. (d) Network of secondary metabolism of identified DEGs between two cultivars at the S3 stage. The orange and green cycles represent up- and down-regulated DEGs in 'OB' compared to 'CH'. The edges connect the DEGs with corresponding pathways.

stem, whereas that of *RcCH_OOMT2* was not detected in any of the six tissues. Aligning the promoter sequences of *OOMT*s genes between 'OB' and 'CH', we found more similarity in the promoter sequences between *RcOB_OOMT1* and *RcCH_OOMT1* (Supplementary Fig. S2) than in that between *RcOB_OOMT2* and *RcCH_OOMT2* (Supplementary Fig. S3). In addition, *RcCH_OOMT2* amino acid sequence was

shorter than that of three *RcOOMT*s and lacked the dimerization domain (Supplementary Fig. S4a).

In the biosynthesis pathway of 2-PE, the expression level of *RcOB_AAAT* (*RcCH_v1.0_chr5.2131*) increased as the flower developed (Fig. 4). Although the expression trend of *RcCH_AAAT* followed a similar pattern to that of *RcOB_AAAT*, the expression level of

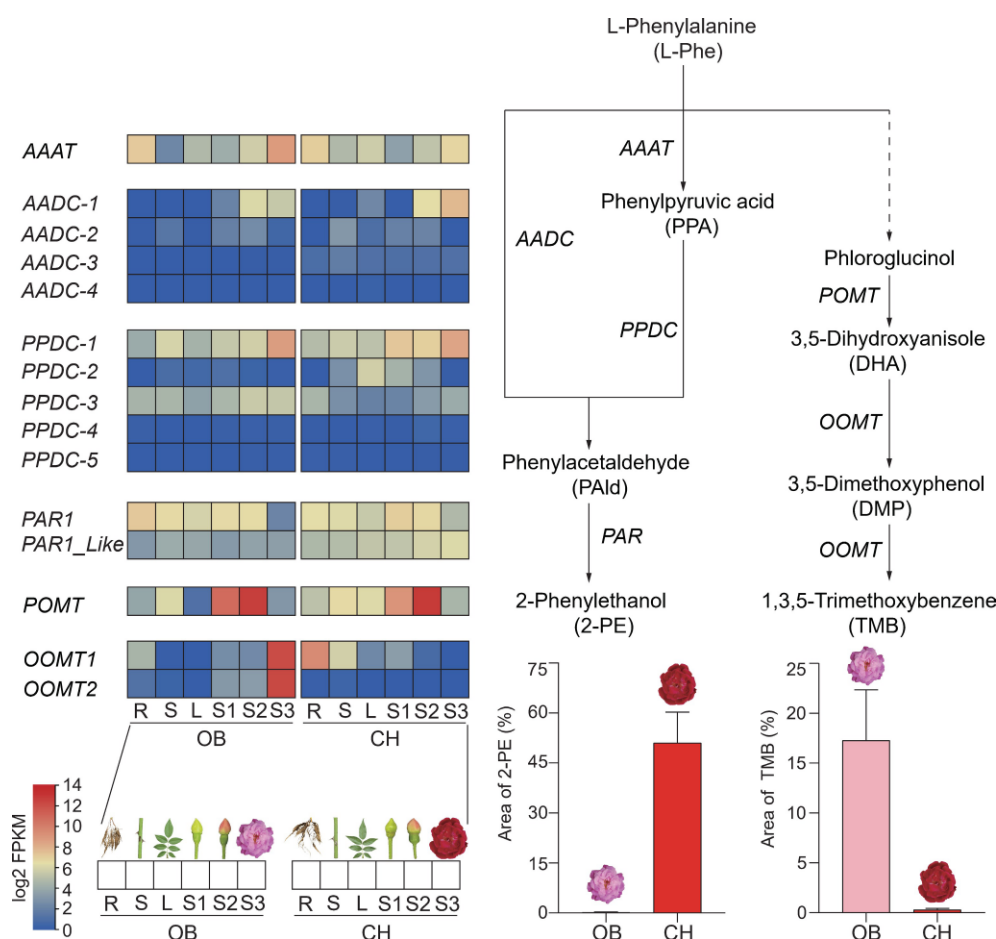


Fig. 4 Metabolomic and transcriptomic analysis of phenylpropanoid synthesis pathways in six tissues of 'OB' and 'CH'. POMT, phloroglucinol O-methyltransferase; OOMT, orcinol O-methyltransferase; AAAT, aromatic amino acid aminotransferase; AADC, aromatic amino acid decarboxylase; PPDC, phenylpyruvic acid decarboxylase; PAR, phenylacetaldehyde reductase; R, root; S, stem; L, leaf.

RcCH_AAAT at the S3 stage was significantly lower than that of *RcOB_AAAT*. Among the five *PPDC* genes identified in the two cultivars, only one gene, *PPDC-1* (*RcCH_v1.0_chr3.1054*), displayed notable expression levels in flowers, indicating a distinct functional role. In an alternative route of 2-PE biosynthesis, the *AADC-1* gene (*RcCH_v1.0_chr6.304*) showed notable increases along with flower development in both cultivars, distinguishing it from the other three *AADC* genes identified in the two cultivars (Fig. 4).

PAR gene plays a critical role in catalyzing the reduction of PALd to 2-PE. The tissue-specific expression pattern of the *RcPAR1* (*RcCH_v1.0_chr5.4505*) gene exhibited a striking similarity between the two cultivars, displaying a gradual decline in root, stem, and leaf, as well as during the stages of flower development. At stage S3, the expression of *RcOB_PAR1* (*RcCH_v1.0_chr5.4505*) was decreased compared to that at the stages S1 and S2, while the expression of *RcOB_PAR1* was notably inferior to that of *RcCH_PAR1*. The expression level of *RcOB_PAR1_Like* (*RcCH_v1.0_chr7.2995*) was found to be similar in all six tissues. *RcCH_PAR1_Like* consistently exhibited higher expression levels compared to *RcOB_PAR1_Like* in all three stages.

Identification of *RcCH_AADC-1* and *RcCH_PARs* genes involved in the synthesis of 2-PE

2-PE plays a crucial role in perfumes, essential oils, and cosmetics, contributing to the reputation of rose as 'liquid gold'^[41]. In this study, we conducted phylogenetic analysis and transient transformation on selected genes, *RcCH_AADC-1* and *RcCH_PARs*, to explore the connection between these genes and 2-PE synthesis (Fig. 5 &

Supplementary Fig. S4b). The *AADC* amino acid sequences from different species showed similar motif structure (Supplementary Fig. S4b). *AADC-3* and *AADC-4* were found to be clustered together in both cultivars, whereas *AADC-1* and *AADC-2* were not. The sequences of *AADC-1* from two cultivars were found to cluster in a group with the reported *RdAADC*, *RhAADC*, and *RhPAAS*.

The genes of *PARs* and *DFRs* were identified as PF01370 on the SDR website (www.sdr-enzymes.org) (Supplementary Table S5). The *PARs* amino acid sequences exhibited conserved motifs (motifs 1 and 2) that are characteristic of the SDRs superfamily, containing the cofactor binding site (TGxxxGxG) and the active site (YxxxK) in both cultivars (Supplementary Fig. S4c). By constructing phylogenetic trees, four *PARs* of 'OB' and 'CH' were divided into two clades (*PAR1* and *1_Like* clades), and orthologous genes from different cultivars clustered into one clade (Fig. 5a). Among them, we found that the amino acid sequences of *RcOB_PAR1* and *RcCH_PAR1* are identical, as well as *RcOB_PAR1_Like* and *RcCH_PAR1_Like*. While the similarity of amino acid sequences between the two *PARs* from the same cultivar was found to be 73.65%.

To clarify the functional characteristics of the highly expressed *RcCH_AADC-1* and *RcCH_PARs*, these genes were overexpressed by the transient transformation of the vectors into tobacco via *A. tumefaciens* (Fig. 5b). The levels of 2-PE in transgenic tobacco leaves were detected by GC-MS. We found that overexpression of *RcCH_AADC-1* can promote the accumulation of 2-PE (Fig. 5c). Furthermore, the co-expression of *RcCH_AADC-1* and *RcCH_PAR1_Like* exhibited the lowest level of 2-PE, while the co-expression of *RcCH_AADC-1* and

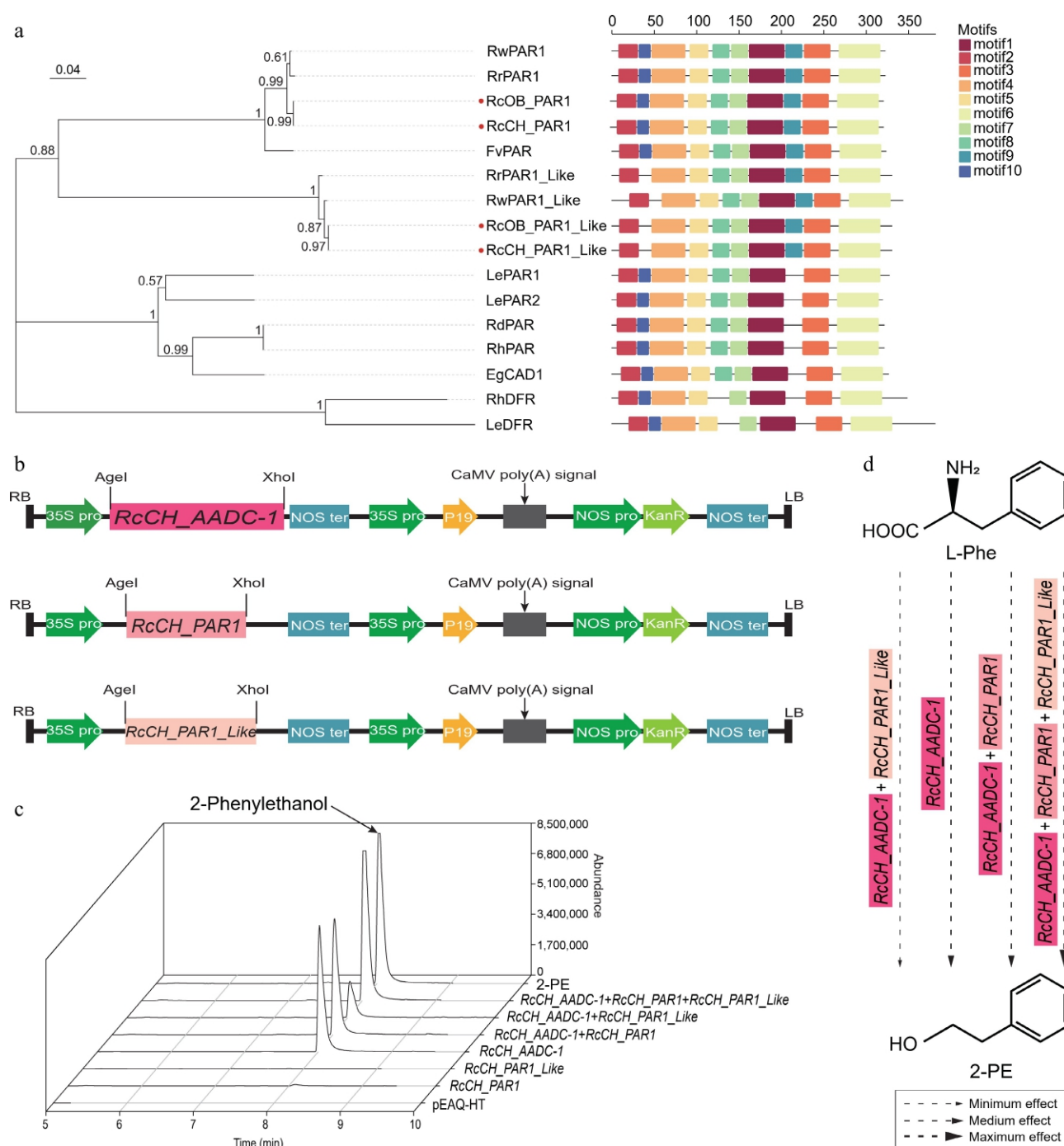


Fig. 5 The characterization of the *RcCH_AADC-1* and *RcCH_PARs* genes. (a) Phylogenetic analysis of PARs from *R. chinensis* and other plants by MEGA. Protein IDs are shown in [Supplementary Table S6](#). (b) Recombinant pEAQ-HT vectors with *RcCH_AADC-1*, *RcCH_PAR1*, and *RcCH_PAR1_Like*. (c) The relative contents of 2-PE in empty pEAQ-HT vector, *RcCH_AADC-1*, and *RcCH_PARs* transgenic lines. (d) The potential 2-PE synthesis pathway. Arrows of different sizes indicate the effect of *RcCH_AADC-1* and *RcCH_PARs* on the formation of 2-PE. Thin, medium, and coarse arrows represent minimum, medium, and maximum effect.

two *RcCH_PARs* resulted in higher content of 2-PE than that of *RcCH_AADC-1* overexpression. In addition, either *RcCH_PAR1* or *RcCH_PAR1_Like* was individually transformed into tobacco plants, we did not detect any significant increase in the level of 2-PE compared with that of the empty vector. Consequently, we proposed a potential model of the pathways governing the biosynthesis of 2-PE that co-expressing *RcCH_PARs* with *RcCH_AADC-1* presented different regulations in the biosynthesis of 2-PE (Fig. 5d).

Discussion

This study investigated two famous *R. chinensis* cultivars 'OB' and 'CH' for an assessment of the reason for differences in floral scent. Because the phenotypic divergence between these two cultivars seemed likely to provide good material for research on floral fragrances. The total content of volatile compounds in 'OB' was significantly lower than that in 'CH', 'OB' possessed more types of terpenoids, and occupied 57% of the total volatiles. Our results indicated that TMB and 2-PE are the most representative volatile

constituents in 'OB' and 'CH' flowers, respectively, which is consistent with previous reports^[4,25]. Combining the transcriptomic and transformation analysis, our findings revealed that *OOMTs* play a crucial role in TMB synthesis and *AADC-1* serves as a pivotal regulator in 2-PE synthesis.

Sequence differences of *RcOOMTs* gene

TMB is a crucial component of the 'Chinese rose odor' as a phenylpropanoid compound^[23,42]. This volatile compound is a potent sedative and has been utilized as an ingredient in cosmetics^[42]. Interestingly, high levels of TMB were specifically detected in the *Chinenses* section of the *Rosa* subgenus, while trace amounts of TMB were found in other sections like *Gymnocarpae*, *Gallicanae*, *Synstylae*, and *Banksianae*^[43]. In this study, there were higher levels of TMB in 'OB' than in 'CH' flowers (Fig. 2b), in line with previous research findings^[6,20]. This indicates that variations in TMB contents are present not only between different sections in *rosa*, but also among *Chinenses* section.

A phylogenetic analysis of the *OOMT* gene family in five Chinese roses and 13 Eurasian rose species revealed that only Chinese roses possess both the *OOMT1* and *OOMT2* genes^[4]. In the present study, both *OOMT1* and *OOMT2* were identified in 'OB' and 'CH' flowers (Fig. 4). The genes *RcOB_OOMT1*, *RcOB_OOMT2*, and *RcCH_OOMT1* contain the dimerization and AdoMet_MTases superfamily domain, and their expression levels changed along with the flower development in both cultivars. *RcCH_OOMT2* only possesses a partial segment of the AdoMet_MTases superfamily domain, and its expression level remained (Fig. 4 & Supplementary Fig. S4a). This suggests that two domains are essential for the function of *OOMT* genes. The *OOMT2* gene may be critical for the biosynthesis of TMB in *R. chinensis*.

Previous research has demonstrated European roses expressed *OOMT* genes in their stamens rather than in flower petals. In contrast, levels of *OOMT1* and *OOMT2* were higher in the petals of Chinese roses instead of in other tissues^[44]. As the key genes in the biosynthesis of TMB, the upregulation of *OOMTs* genes can promote the synthesis of TMB in roses. In our study, *RcOB_OOMTs* were specifically expressed in full blooming 'OB' petals (S3). While in 'CH', minimal levels of *RcCH_OOMT1* were observed in S1 and S2 petals, *RcCH_OOMT2* showed no detectable mRNA transcripts in petals (Fig. 4). The finding suggests that the development of TMB biosynthesis in Chinese roses relies on the concurrent expression of *OOMT1* and *OOMT2*, accompanied by an upregulation of *OOMT* expression in petals.

Functional differentiation of *RcPARs* genes

The 2-PE is a prevalent scent compound abundantly emitted by rose flowers, contributing to its characteristic rose-like scent^[25]. As the predominant component commonly present in perfumes and essential oils, the 2-PE is usually extracted from the Damask rose^[20]. Universally, L-Phe is gradually converted into 2-PE through the catalytic action of *AADC* and *PAR*^[24]. After overexpressing *RcCHAADC-1* in tobacco leaves, a high level of 2-PE was noticed (Fig. 5), which reinforces the previous findings that modulating *AADC* expression can influence the synthesis of phenylalanine-based aroma volatiles in *R. rugosa* and *R. hybrida*^[29,45]. A previous study showed that the reduction of PAld to 2-PE can be catalyzed by *PAR* or alcohol dehydrogenase (*ADH*)^[26]. Therefore, it cannot be ruled out that endogenous dehydrogenase (e.g., *ADH*) in tobacco may replace *PAR* in the reduction reaction. The upregulation of *RcCH_AADC-1* gene expression might serve as a key factor in 2-PE synthesis in roses.

PAR functions as the key enzyme in the last step of 2-PE biosynthesis^[26]. *PAR* gene has one copy in *R. rugosa* 'Tanghong'^[41], *R. damascene*^[17], and *R. hybrida* 'Yves Piaget'^[46]. The expression of

RdPAR, *RrPAR*, and *LePARs* increased consistently from the budding stage to the half-opening stage, and decreased at the full-opening stage^[17,28,41]. In our study, two *PAR* genes were identified in both cultivars, one was *PAR1*, whose expression pattern was consistent with previous reports^[17,28,41]. The other one is *PAR1_Like*, whose expression pattern was not. In 'OB', *RcOB_PAR1_Like* was lowly expressed at the three stages of petal, while *RcCH_PAR1_Like* expression increased from S1 to S3 in 'CH' (Fig. 4). In the presence of nicotinamide adenine dinucleotide phosphate (NADPH) or nicotinamide adenine dinucleotide (NADH), *PAR* efficiently converted PAld to 2-PE^[17,26]. This may explain to why neither overexpression of *RcPAR1* nor *RcPAR1_Like* independently regulated 2-PE synthesis in this study. It is also possible that the PAld contents in tobacco may not be sufficient to synthesize more 2-PE. In addition, the analysis of sequences, evolutionary trees, and transient transformation of *RcPAR1* and *RcPAR1_Like* revealed the functional diversity in these genes. When one *RcPAR* copy was co-expressed with *RcAADC-1*, it exhibited significantly lower levels of 2-PE compared to the situation where two *RcPARs* were co-expressed with *RcAADC-1*. Hence, the functional differentiation of *RcPAR1* and *RcPAR1_Like*, along with their involvement in the regulatory mechanisms of 2-PE formation, requires further investigation.

Conclusions

This study investigated the floral fragrances in the blooming flower of two *R. chinensis* cultivars. The main specific focus on essential volatile floral components were identified: TMB in 'OB' and 2-PE in 'CH'. In addition, 15 key genes involved in the biosynthesis of phenylpropanoid were identified in *R. chinensis* flowers by analysis of transcriptome data. For example, *RcOOMTs* are involved in the synthesis of TMB, *RcPARs* and *RcAADC-1* are involved in the synthesis of 2-PE. Transgenic experiments suggested that *RcAADC-1* gene acts as a pivotal regulator in the biosynthesis of 2-PE. These findings provide valuable insight for practical production of rose essential oils.

Author contributions

The authors confirm contribution to the paper as follows: study conception: Zhang X, Wu Z; methodology: Luo K, Song C, Huang R, Leng L; investigation: Luo K; formal analysis: Luo K, Song C, Liao X; data curation: Song C, Yang Y, Leng L, Gu C; validation: Bao T; writing - original draft: Luo K, Song C; writing - review & editing: Luo K, Song C, Bao T, Lin S, Zhang X, Wu Z; supervision: Zhang X, Wu Z; funding acquisition, project administration: Wu Z. All authors reviewed the results and approved the final version of the manuscript.

Data availability

All data generated or analyzed during this study are included in this published article and its supplementary information files.

Acknowledgments

This work was supported in part by the Chinese Academy of Agricultural Sciences Elite Youth Program to Zhiqiang Wu; and this work was also supported by funding from the Scientific Research Foundation for Principle Investigator, Kunpeng Institute of Modern Agriculture at Foshan (KIMA-QD2022004); the Funding of Major Scientific Research Tasks, Kunpeng Institute of Modern Agriculture at Foshan (KIMA-ZDKY2022004); and Foshan self-funded scientific

and technological innovation projects (2320001007191). We thank members of the Wu laboratory. We thank Prof. Li Wei (Agricultural Genomics Institute at Shenzhen, Chinese Academy of Agricultural Sciences) for providing the pEAQ-HT vector.

Conflict of interest

The authors declare that they have no conflict of interest.

Supplementary information accompanies this paper at (<https://www.maxapress.com/article/doi/10.48130/opr-0025-0003>)

Dates

Received 3 September 2024; Revised 21 November 2024; Accepted 25 December 2024; Published online 4 March 2025

References

- Bendahmane M, Dubois A, Raymond O, Le Bris M. 2013. Genetics and genomics of flower initiation and development in roses. *Journal of Experimental Botany* 64:847–57
- Başer H, Altıntaş A, Kurkuoğlu M. 2013. Turkish rose. A review of the history, ethnobotany and modern uses of rose petals, rose oil, rose water and other rose products. *HerbalGram* 96:40–53
- Mileva M, Ilieva Y, Jovtchev G, Gateva S, Zaharieva MM, et al. 2021. Rose flowers—a delicate perfume or a natural healer? *Biomolecules* 11:127
- Scalliet G, Piola F, Douady CJ, Rety S, Raymond O, et al. 2008. Scent evolution in Chinese roses. *Proceedings of the National Academy of Sciences of the United States of America* 105:5927–32
- Zhou L, Wu S, Chen Y, Huang R, Cheng B, et al. 2024. Multi-omics analyzes of *Rosa gigantea* illuminate tea scent biosynthesis and release mechanisms. *Nature Communications* 15:8469
- Zhou L, Yu C, Cheng B, Han Y, Luo L, et al. 2020. Studies on the volatile compounds in flower extracts of *Rosa odorata* and *R. chinensis*. *Industrial Crops and Products* 146:112143
- Kigathi RN, Unsicker SB, Reichelt M, Kesselmeier J, Gershenzon J, et al. 2009. Emission of volatile organic compounds after herbivory from *Trifolium pratense* (L.) under laboratory and field conditions. *Journal of Chemical Ecology* 35:1335–48
- Muhlemann JK, Klempien A, Dudareva N. 2014. Floral volatiles: from biosynthesis to function. *Plant, Cell & Environment* 37:1936–49
- Ibrahim M, Agarwal M, Hardy G, Ren Y. 2017. Optimized method to analyze rose plant volatile organic compounds by HS-SPME-GC-FID/MSD. *Journal of Biosciences and Medicines* 5:13–31
- Dudareva N, Klempien A, Muhlemann JK, Kaplan I. 2013. Biosynthesis, function and metabolic engineering of plant volatile organic compounds. *New Phytologist* 198:16–32
- Dudareva N, Cseke L, Blanc VM, Pichersky E. 1996. Evolution of floral scent in *Clarkia*: novel patterns of S-linalool synthase gene expression in the *C. breweri* flower. *The Plant Cell* 8:1137–48
- Guterman I, Shalit M, Menda N, Piestun D, Dafny-Yelin M, et al. 2002. Rose scent: genomics approach to discovering novel floral fragrance-related genes. *The Plant Cell* 14:2325–38
- Dudareva N, Martin D, Kish CM, Kolosova N, Gorenstein N, et al. 2003. (*E*)- β -ocimene and myrcene synthase genes of floral scent biosynthesis in snapdragon: function and expression of three terpene synthase genes of a new terpene synthase subfamily. *The Plant Cell* 15:1227–41
- Nagegowda DA, Gutensohn M, Wilkerson CG, Dudareva N. 2008. Two nearly identical terpene synthases catalyze the formation of nerolidol and linalool in snapdragon flowers. *The Plant Journal* 55:224–39
- Ginglinger JF, Boachon B, Höfer R, Paetz C, Köllner TG, et al. 2013. Gene coexpression analysis reveals complex metabolism of the monoterpene alcohol linalool in *Arabidopsis* flowers. *The Plant Cell* 25:4640–57
- Kaminaga Y, Schnepf J, Peel G, Kish CM, Ben-Nissan G, et al. 2006. Plant phenylacetaldehyde synthase is a bifunctional homotetrameric enzyme that catalyzes phenylalanine decarboxylation and oxidation. *The Journal of Biological Chemistry* 281:23357–66
- Chen XM, Kobayashi H, Sakai M, Hirata H, Asai T, et al. 2011. Functional characterization of rose phenylacetaldehyde reductase (PAR), an enzyme involved in the biosynthesis of the scent compound 2-phenylethanol. *Journal of Plant Physiology* 168:88–95
- Koeduka T, Fujita Y, Furuta T, Suzuki H, Tsuge T, et al. 2017. Aromatic amino acid decarboxylase is involved in volatile phenylacetaldehyde production in loquat (*Eriobotrya japonica*) flowers. *Plant Biotechnology* 34:193–98
- Lavid N, Wang J, Shalit M, Guterman I, Bar E, et al. 2002. O-methyltransferases involved in the biosynthesis of volatile phenolic derivatives in rose petals. *Plant Physiology* 129:1899–907
- Scalliet G, Journot N, Jullien F, Baudino S, Magnard JL, et al. 2002. Biosynthesis of the major scent components 3,5-dimethoxytoluene and 1,3,5-trimethoxybenzene by novel rose O-methyltransferases. *FEBS Letters* 523:113–18
- Wang J, Pichersky E. 1998. Characterization of S-adenosyl-L-methionine: (Iso)eugenol O-methyltransferase involved in floral scent production in *Clarkia breweri*. *Archives of Biochemistry and Biophysics* 349:153–60
- Koksai N, Saribas R, Kafkas E, Aslançan H, Sadighzadeh S. 2015. Determination of volatile compounds of the first rose oil and the first rose water by HS-SPME/GC/MS techniques. *African Journal of Traditional Complementary and Alternative Medicines* 12:145–50
- Jochi A, Yomogida K, Awano KI, Ueda Y. 2005. Volatile components of tea-scented modern roses and ancient Chinese roses. *Flavour and Fragrance Journal* 20:152–57
- Hirata H, Ohnishi T, Ishida H, Tomida K, Sakai M, et al. 2012. Functional characterization of aromatic amino acid aminotransferase involved in 2-phenylethanol biosynthesis in isolated rose petal protoplasts. *Journal of Plant Physiology* 169:444–51
- Hirata H, Ohnishi T, Watanabe N. 2016. Biosynthesis of floral scent 2-phenylethanol in rose flowers. *Bioscience, Biotechnology, and Biochemistry* 80:1865–73
- Sakai M, Hirata H, Sayama H, Sekiguchi K, Itano H, et al. 2007. Production of 2-phenylethanol in roses as the dominant floral scent compound from L-phenylalanine by two key enzymes, a PLP-dependent decarboxylase and a phenylacetaldehyde reductase. *Bioscience, Biotechnology, and Biochemistry* 71:2408–19
- Tieman D, Taylor M, Schauer N, Fernie AR, Hanson AD, et al. 2006. Tomato aromatic amino acid decarboxylases participate in synthesis of the flavor volatiles 2-phenylethanol and 2-phenylacetaldehyde. *Proceedings of the National Academy of Sciences of the United States of America* 103:8287–92
- Tieman DM, Loucas HM, Kim JY, Clark DG, Klee HJ. 2007. Tomato phenylacetaldehyde reductases catalyze the last step in the synthesis of the aroma volatile 2-phenylethanol. *Phytochemistry* 68:2660–69
- Sheng L, Zeng Y, Wei T, Zhu M, Fang X, et al. 2018. Cloning and functional verification of genes related to 2-phenylethanol biosynthesis in *Rosa rugosa*. *Genes* 9:576
- Han Y, Wan H, Cheng T, Wang J, Yang W, et al. 2017. Comparative RNA-seq analysis of transcriptome dynamics during petal development in *Rosa chinensis*. *Scientific Reports* 7:43382
- Zhang X, Wu Q, Lan L, Peng D, Guan H, et al. 2024. Haplotype-resolved genome assembly of the diploid *Rosa chinensis* provides insight into the mechanisms underlying key ornamental traits. *Molecular Horticulture* 4:14
- Zhao CY, Xue J, Cai XD, Guo J, Li B, et al. 2016. Assessment of the key aroma compounds in rose-based products. *Journal of Food and Drug Analysis* 24:471–76
- Bolger AM, Lohse M, Usadel B. 2014. Trimmomatic: a flexible trimmer for Illumina sequence data. *Bioinformatics* 30:2114–20
- Kim D, Paggi JM, Park C, Bennett C, Salzberg SL. 2019. Graph-based genome alignment and genotyping with HISAT2 and HISAT-genotype. *Nature Biotechnology* 37:907–15
- Pertea M, Pertea GM, Antonescu CM, Chang TC, Mendell JT, et al. 2015. StringTie enables improved reconstruction of a transcriptome from RNA-seq reads. *Nature Biotechnology* 33:290–95

36. Anders S, Pyl PT, Huber W. 2015. HTSeq—a Python framework to work with high-throughput sequencing data. *Bioinformatics* 31:166–69
37. Chen C, Wu Y, Li J, Wang X, Zeng Z, et al. 2023. TBtools-II: a "one for all, all for one" bioinformatics platform for biological big-data mining. *Molecular Plant* 16:1733–42
38. Xie J, Chen Y, Cai G, Cai R, Hu Z, et al. 2023. Tree Visualization By One Table (tvBOT): a web application for visualizing, modifying and annotating phylogenetic trees. *Nucleic Acids Research* 51:W587–W592
39. Sainsbury F, Thuenemann EC, Lomonosoff GP. 2009. pEAQ: versatile expression vectors for easy and quick transient expression of heterologous proteins in plants. *Plant Biotechnology Journal* 7:682–93
40. Zhou L, Yu C, Cheng B, Wan H, Luo L, et al. 2020. Volatile compound analysis and aroma evaluation of tea-scented roses in China. *Industrial Crops and Products* 155:112735
41. Feng L, Wang M, Wang J, Zang S, Xia W, et al. 2015. Isolation of 2-phenylethanol biosynthesis related genes and their relationship with 2-phenylethanol accumulation in *Rosa rugosa*. *Acta Physiologiae Plantarum* 37:256
42. Wu S, Watanabe N, Mita S, Dohra H, Ueda Y, et al. 2004. The key role of phloroglucinol O-methyltransferase in the biosynthesis of *Rosa chinensis* volatile 1,3,5-trimethoxybenzene. *Plant Physiology* 135:95–102
43. Noh YM, Ait Hida A, Raymond O, Comte G, Bendahmane M. 2024. The scent of roses, a bouquet of fragrance diversity. *Journal of Experimental Botany* 75:1252–64
44. Scalliet G, Lionnet C, Le Behec M, Dutron L, Magnard JL, et al. 2006. Role of petal-specific orcinol O-methyltransferases in the evolution of rose scent. *Plant Physiology* 140:18–29
45. Rocchia A, Hibrand-Saint Oyant L, Cavel E, Caissard JC, Machenaud J, et al. 2019. Biosynthesis of 2-phenylethanol in rose petals is linked to the expression of one allele of *RhPAAS*. *Plant Physiology* 179:1064–79
46. Chen X, Baldermann S, Cao S, Lu Y, Liu C, et al. 2015. Developmental patterns of emission of scent compounds and related gene expression in roses of the cultivar *Rosa x hybrida* cv. 'Yves Piage'. *Plant Physiology and Biochemistry* 87:109–14



Copyright: © 2025 by the author(s). Published by Maximum Academic Press, Fayetteville, GA. This article is an open access article distributed under Creative Commons Attribution License (CC BY 4.0), visit <https://creativecommons.org/licenses/by/4.0/>.